JOURNAL OF SOLID STATE CHEMISTRY **71**, 189–195 (1987)

New Double Chloride in the LiCl–CoCl$_2$ System

I. Preparation, Crystal Structure, Phase Transformation, and Ionic Conductivity of Li$_6$CoCl$_8$

R. KANNO,* Y. TAKEDA, A. TAKAHASHI, AND O. YAMAMOTO

Department of Chemistry, Faculty of Engineering, Mie University, Tsu, 514 Japan

R. SUYAMA†

College of General Education, Osaka University, Osaka, 560 Japan

AND M. KOIZUMI

Institute of Scientific and Industrial Research, Osaka University, Osaka, 565 Japan

Received July 22, 1986; in revised form December 5, 1986

The phase diagram of the LiCl–CoCl$_2$ system has been determined by X-ray diffraction and differential thermal analysis. The system contains two intermediate compounds, Li$_6$CoCl$_8$, with the Mg$_6$MnO$_8$-type structure, and Li$_2$CoCl$_4$, with a related spinel structure. The crystal structure of Li$_6$CoCl$_8$ was determined by X-ray powder Rietveld refinement at room temperature. This phase has the Mg$_6$MnO$_8$-type structure with ordered cations and vacancy arrangement over octahedral sites, and its cubic lattice parameter is $a = 10.2584(3)$ Å. Li$_6$CoCl$_8$ turns reversibly into the LiCl-type structure at 350°C. The electrical conductivity measurements showed a high ionic conductivity of 9.3×10^{-2} S cm^{-1} at 400°C. © 1987 Academic Press, Inc.

Introduction

Lithium ion conductors have received considerable attention during the past decade as electrolyte materials for solid lithium batteries. Recently, the intermediate compounds in the LiCl–MCl$_2$ (M = Mg, V, Mn, Fe, Cd) system have been studied from the standpoint of high lithium ion conductivity (*1–5*). The chloride spinels Li$_2M$Cl$_4$ (M = Mg, V, Mn, Fe, Cd), reported to have the inverse spinel structure (*6*), showed a high lithium ion conductivity of around 0.1 S cm^{-1} at 400°C. The values of the conductivity at elevated temperatures are comparable to or greater than those for the high lithium ion conductors reported previously. The formation of intermediate compound with a formula Li$_6$MCl$_8$ has been reported only in the LiCl–VCl$_2$ system (*7*). Li$_6$VCl$_8$ has the Mg$_6$MnO$_8$-type structure, which is isostructural with the so-called Suzuki-type phase. It corresponds to a super-

---

* To whom correspondence should be addressed.

† Present address: Shinnippon Steel Corp., Central R & D Bureau, R & D Laboratories-1, Materials Research Lab.-1, Kawasaki, Japan.

0022-4596/87 $3.00

structure of LiCl, where the cations and vacancies are ordered in the cation sublattice. Measurement of NMR (*8*) confirmed the lithium ion mobility with the activation energy of ~40 kJ mole^{-1}.

Whereas the intermediate compounds such as Li_2MCl_4 and Li_6MCl_8 were well characterized in the $LiCl–MCl_2$ (M = Mg, V, Mn, Fe, Cd) system, neither the spinel nor the Suzuki-type phase has been reported for the $LiCl–CoCl_2$ system. The phase diagram of the system was constructed using differential thermal analysis (DTA) measurements by von Seifert (*9*) in 1961. Three intermediate phases, Li_4CoCl_6, Li_2CoCl_4, and $LiCoCl_3$, were suggested. The precise structural study, however, has not yet been reported. This may be due to difficulties in identifying reaction products, the X-ray patterns of which showed a close resemblance to those of the starting materials. The difficulties arise also from a slight structural distortion of the intermediate compound as described in a later part of this paper. Nevertheless, the double cobalt chlorides containing lithium would be expected to have high ionic conductivity by analogy to other chlorides.

The purpose of the present study is to confirm the intermediate phases in the $LiCl–CoCl_2$ system and to measure their electrical properties. To obtain the conclusive phase relation, we prepared more than 30 different samples, analyzing them with a powerful X-ray diffractometer, a high-temperature X-ray diffractometer, and a DTA measurement. As a result, we confirmed two intermediate compounds, Li_6CoCl_8, with the Mg_6MnO_8-type structure, and Li_2CoCl_4, with a related spinel structure. Both compounds have high ionic conductivity at higher temperatures and show the transition from the low to high conducting state. We report here the phase diagram of the $LiCl–CoCl_2$ system. Further, the structure, the phase transition, and the ionic conductivity of Li_6CoCl_8 are also reported. Li_2CoCl_4 with a related spinel structure will be reported in a forthcoming paper (*10*).

Experimental

Lithium chloride and cobalt dichloride were anhydrous materials (Nakarai Co., >99% purity). They were carefully dried under vacuum (~1 Pa) at 300°C. The melting points of these chlorides were in good agreement with the reported values. The appropriate quantities of LiCl and $CoCl_2$ were ground together and were pressed into a pellet at 60 MPa in a nitrogen-filled glove box. The pellets were then heated in an evacuated Pyrex tube at 400°C for 1 week. X-ray diffraction patterns of the powdered samples were obtained using monochromated Cu$K\alpha$ radiation and a scintillation detector. A high-power X-ray powder diffractometer (Rigaku RAD 12kW) was also used to determine the intermediate compounds. A sample holder has an aluminum window 7 μm thick to prevent attack by moisture during the measurement.

X-ray powder diffraction data for Rietveld analysis were collected on the polycrystalline sample of Li_6CoCl_8 with Cu$K\alpha$ radiation using a high-power X-ray powder diffractometer equipped with a graphite monochromator. The sample was kept under He atmosphere during measurement. Diffraction data were collected by step scanning over an angular range of $10° < 2\theta < 100°$ in increments of 0.02° at room temperature.

The structural refinement of X-ray data was performed using the Rietveld analysis computer program RIETAN provided by Izumi (*11*). All computations were carried out at the Crystallographic Research Center, Institute of Protein Research, Osaka University. Reflection positions and intensities were calculated for both Cu$K\alpha_1$ (λ = 1.5405 Å) and Cu$K\alpha_2$ (λ = 1.5443 Å) with a factor of 0.5 applied to the latter's calculated integrated intensities. The profile function was a pseudo-Voigt function with the mixing parameter γ included in the least-squares refinement.

The high-temperature phases were examined using a high-temperature X-ray diffractometer. The diffraction patterns were taken in a dry nitrogen atmosphere. Silicon powder was used as an internal standard to determine the lattice parameters. Differential thermal analysis was carried out for the samples sealed in silica glass containers under vacuum. α-Al_2O_3 was used as a standard. The heating and cooling rates were 1.5°C/min.

The electrical conductivities were measured in the temperature range between room temperature and 500°C in a dry argon gas flow. A sample of about 0.5 g was pressed into pellets. Blocking electrodes were deposited on both sides on the pellets by evaporating gold. The conductivity was obtained by ac impedance measurement using a HP4800A vector impedance meter over a frequency range of 5 Hz–500 kHz.

Experimental Results and Discussion

Phase Diagram of the LiCl–CoCl₂ System

We constructed the phase diagram, shown in Fig. 1, using X-ray diffraction and DTA measurements in order to characterize phases existing in the system. The X-ray diffraction data were studied for the samples prepared at 5 mole% intervals and also for 14.3 mole% $CoCl_2$ (Li_6CoCl_8) and 33.3 mole% $CoCl_2$ (Li_2CoCl_4). A reinvestigation of this system confirmed two intermediate compounds, Li_6CoCl_8 and Li_2CoCl_4. The X-ray pattern of the sample containing 14.3 mole% $CoCl_2$ (Li_6CoCl_8) showed a striking resemblance to that of lithium chloride. However, some extra lines which could not be indexed by LiCl were observed. Intensity of the extra lines increased linearly with $CoCl_2$ content from 0 to 14.3 mole%. The samples containing more than 14.3 mole% $CoCl_2$ showed additional diffraction lines. These results indicate the existence of an intermediate compound with a formula of Li_6CoCl_8.

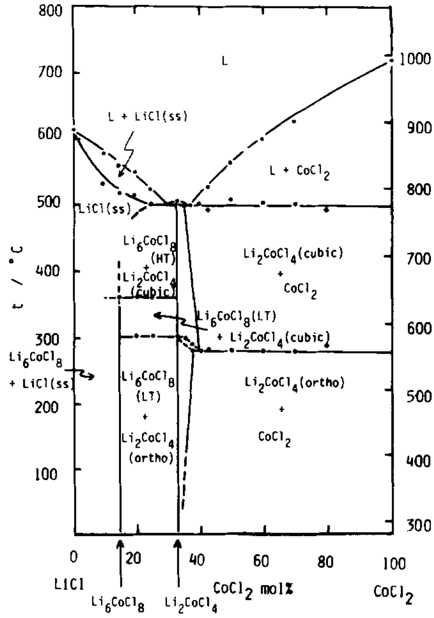

FIG. 1. Phase diagram of the LiCl–$CoCl_2$ system. HT and LT indicate the high- and low-temperature phases, respectively.

The samples containing 14.3–33.3 mole% $CoCl_2$ showed extra X-ray diffraction lines which could not be indexed by Li_6CoCl_8. The lines due to $CoCl_2$ were not observed in the samples containing less than 33.3 mole% $CoCl_2$ (Li_2CoCl_4). The intensity of the extra lines such as d = 2.569 and 1.794 Å increased in proportion to $CoCl_2$ content, and the maximum intensity was observed in the sample with 33.3 mole% $CoCl_2$. These results indicate the existence of an intermediate compound with the content of 33.3 mole% $CoCl_2$ (Li_2CoCl_4). The diffraction pattern of Li_2CoCl_4 showed a strong resemblance to the cubic chloride spinels Li_2MCl_4 (M = Mg, Mn, Fe, Cd). Some lines, however, partially split into doublets. The precise structural description of Li_2CoCl_4 will be reported in a forthcoming paper (*10*).

TABLE I

RIETVELD REFINEMENT RESULTS FOR Li_6CoCl_8

Scale factor	0.00859(7)
FWHM parameter U	0.268(26)
V	−0.154(19)
W	0.064(4)
Asymmetry parameter	0.129(25)
Gaussian fraction	0.381(22)
FWHM (Gauss)/FWHM (Lorentz)	1.66(8)
Lattice constant a (Å)	10.2584(3)

			Fractional coordinates			
Atom	Site	Occupancy	x	y	z	B (Å^2)
Li	24*d*	1	0	0.25	0.25	0.3(14)
Co	4*a*	1	0	0	0	1.9(6)
Cl(1)	8*c*	1	0.25	0.25	0.25	1.9(6)
Cl(2)	24*e*	1	0.243(1)	0	0	1.4(3)

Li_2CoCl_4 melts congruently at 505°C. The eutectic points are shown at 500°C around both 30 and 38 mole% $CoCl_2$.

X-Ray Characterization of Li_6CoCl_8

All the diffraction lines of Li_6CoCl_8 were indexed by a cubic unit cell with $a = 10.26$ Å, which is a factor of two larger than the unit cell of LiCl, $a = 5.1396$ Å. Diffraction extinctions (*hkl* present only with $h + k$, $k + l$, $l + h = 2n$, $0kl$ only with $k, l = 2n$, hhl only with $h + l = 2n$, $h00$ only with $h = 2n$) were characteristic of space group $Fm3m$. The pattern showed a close resemblance to that of Li_6VCl_8 which is isostructural with the so-called Suzuki phase, Na_6MCl_8 (M = Mg, Mn, Fe, Cd) (*7*, *12*). The structure of Na_6MCl_8 was determined to be isostructural with the double oxide Mg_6MnO_8 using a neutron diffraction method (*13*). This corresponds to a superstructure of the LiCl-type structure with an ordered arrangement of cations and vacancies over octahedral sites. Divalent metal ions situated in the origin of the cell form the unit cell, and the vacancy is in the body center of the cell. Sodium ions are placed in the 24 octahedral sites, and the chloride ions form the cubic close packing with the u parameter about $\frac{1}{4}$. Each position is shown as follows:

4*a* *M*	0, 0, 0
4*b* Vacant site	$\frac{1}{2}, \frac{1}{2}, \frac{1}{2}$
24*d* Na	$0, \frac{1}{4}, \frac{1}{4}; \frac{1}{4}, 0, \frac{1}{4}; \frac{1}{4}, \frac{1}{4}, 0;$ $0, \frac{1}{4}, \frac{3}{4}; \frac{3}{4}, 0, \frac{1}{4}; \frac{1}{4}, \frac{3}{4}, 0$
8*c* Cl(1)	$\frac{1}{4}, \frac{1}{4}, \frac{1}{4}; \frac{3}{4}, \frac{3}{4}, \frac{3}{4}$
24*e* Cl(2)	$u, 0, 0; 0, u, 0; 0, 0, u;$ $-u, 0, 0; 0, -u, 0;$ $0, 0, -u.$

Rietveld refinement of the structure of Li_6CoCl_8 proceeded in a straightforward manner. Initial coordinates for all atoms were taken as those of the Mg_6MnO_8-type structure as pointed out above. The refinement was done in stages: the atomic coordinates and thermal parameters were fixed in the initial calculations and subsequently allowed to vary only after the scale, background, half-width, and unit cell parameters were close to convergence on their optimum values. The final structural parameters are presented in Table I. Refinement proceeded to the agreement factors $R_{wp} = 29.50$, $R_p = 24.92$, and $R_B = 27.56$. (The agreement factors are based on weighted profile fits, profile fits, and Bragg intensities, respectively.) For further refinement, we assumed the extra conditions that the Co^{2+} ions or Li^+ ions are partially disordered: the disorder for the Co^{2+} ions on the 4*a* and 4*b* vacant sites and on the 4*a* and 24*d* lithium sites, and for the Li^+ ions on the 24*d* and 4*b* vacant sites. Better agreement factors, however, could not be obtained using the above hypotheses. Table II shows bond distances and angles for Li_6CoCl_8 calculated from the X-ray refinement results listed in Table I.

Li_6CoCl_8 has the superstructure of the LiCl-type structure with the ordered arrangement of cations and vacancies over octahedral sites. The $CoCl_6$ octahedra are isolated from each other in the structure. The cubic close packing of the chloride ions is slightly distorted with the positional u parameter of 0.243. ($u = \frac{1}{4}$ corresponds to the ideal cubic close packing.)

TABLE II

BOND LENGTHS AND ANGLES FOR Li_6CoCl_8

	Distance or angle (Å or degree)
Lithium–chlorine octahedron	
Li–Cl(1) (×2)	2.5646(1)
Li–Cl(2) (×4)	2.5654(3)
Cl(1)–Li–Cl(2) (×8)	90
Cl(2)–Li–Cl(2) (×2)	87.1(3)
Cl(2)–Li–Cl(2) (×2)	92.8(3)
Cl(1)–Li–Cl(1)	180
Cl(2)–Li–Cl(2) (×2)	180
Cobalt–chlorine octahedron	
Co–Cl(2) (×6)	2.499(12)
Cl(1)–Co–Cl(1) (×12)	90
Cl(1)–Co–Cl(1) (×3)	180

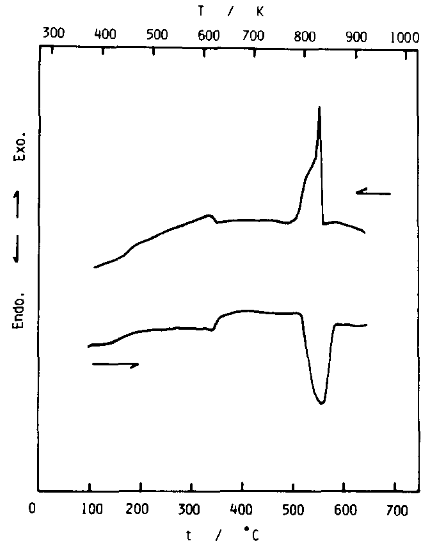

FIG. 3. DTA curves of Li_6CoCl_8.

Electrical Conductivity and Phase Transition

The temperature dependence of the conductivity, σ, of Li_6CoCl_8 is shown in Fig. 2. This phase was found to have high ionic conductivity particularly at higher temperatures. The Arrhenius plots show a change in slope around 360°C. The activation energies were calculated to be 82 kJ $mole^{-1}$ below the knee, and 36 kJ $mole^{-1}$ above the knee in conductivity curve. The conductivity of the Suzuki-type phase Li_6CoCl_8 ($\sigma = 9.3 \times 10^{-2}$ S cm^{-1} at 400°C) is higher than that of lithium chloride ($\sigma = 1.6 \times 10^{-5}$ S cm^{-1} at 400°C (*14*)). These results are consistent with the previous results on Li_6VCl_8 that the introduction of 12.5% cation vacancies in the LiCl structure increased the lithium ion mobility with respect to that of "stoichiometric" LiCl. The Suzuki-type phase Na_6CdCl_8 was also reported to have higher conductivity than that of the stoichiometric compound NaCl (*15*).

Figure 3 shows the DTA curves for Li_6CoCl_8, where the endothermic peak was observed at 350°C on heating. X-ray diffraction patterns at higher temperatures showed that some lines, such as (111), (200), and (311), vanished at 350°C and that the LiCl-type superstructure turned reversibly into the LiCl-type structure. It corresponds to a structural change from the superstructure of LiCl with perfect ordering between cations and vacancies to a disor-

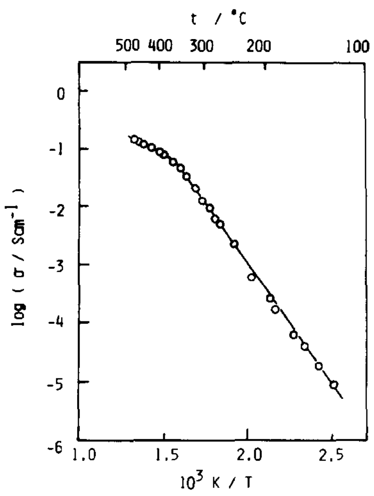

FIG. 2. Temperature dependence of the conductivity of Li_6CoCl_8.

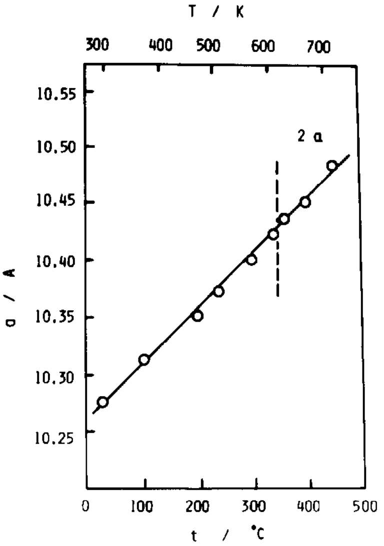

FIG. 4. Temperature dependence of the lattice parameter for Li_6CoCl_8.

dered structure. The reversible phase change of the Suzuki-type phase was also reported for Li_6VCl_8 (*7*).

Figure 4 shows the temperature dependence of the lattice parameter *a* of Li_6CoCl_8. The lattice parameter of the LiCl-type structure is multiplied by a factor of 2 and plotted in the same figure. The lattice parameter increases linearly with temperature and no change in slope was observed around 350°C. The break point in the conductivity curve around 350°C corresponds to the change in cation arrangement from an ordered to a disordered state. The previous conductivity measurements on the Suzuki-type phases Na_6CdCl_8 (*15*) and Li_6VCl_8 (*16*) did not reveal high ionic conduction for the high-temperature disordered phase. The lower activation energy observed for high-temperature Li_6CoCl_8 confirmed that the cation arrangement on the octahedral sites may play an important role for ionic motion. Our result is consistent with the NMR data on Li_6VCl_8 that the ordered phase had higher activation energy (E = 36.7 kJ mole^{-1}) that the disordered one (E = 24.1 kJ mole^{-1}) (*8*). The values of activation energies on NMR, however, are smaller than those obtained by conductivity measurements in this study (E = 82 and 36 kJ mole^{-1} for low- and high-temperature phases, respectively).

The smooth change in slopes in the conductivity curves was also shown in the chloride spinels Li_2MCl_4 (*1–5*). The activation energy decreased above the break point, which corresponds to the structural change from the low to high conduction state (*17*). For the Suzuki-type phase Li_6CoCl_8, the lower activation energy above the break point in the conductivity curve indicates that the transition from the ordered to disordered cation distribution phase also corresponds to the transition from a low to high conducting state.

Acknowledgments

Reflection intensity measurements were performed at the Materials Analyzing Center at the Institute of Scientific and Industrial Research, Osaka University. We thank Mr. Tanaka of the Center for his assistance on the measurement. We thank Professors K. Kamiya and T. Yoko at Mie University for the use of the high-temperature X-ray diffractometer. We also thank Dr. C. Cros of Laboratoire de Chimie du Solide du CNRS at Bordeaux University for useful discussions on the Suzuki-type phase and Professor S. Kume of College of General Education at Osaka University for useful discussions.

References

1. R. KANNO, Y. TAKEDA, AND O. YAMAMOTO, *Mater. Res. Bull.* **16,** 999 (1981).
2. H. D. LUTZ, W. SCHMIDT, AND H. HAEUSELER, *J. Phys. Chem. Solids* **42,** 287 (1981).
3. C. CROS, L. HANEBALI, L. LATIE, G. VILLENEUVE, AND W. GANG, *Solid State Ionics* **9/10,** 139 (1983).
4. R. KANNO, Y. TAKEDA, AND O. YAMAMOTO, *Solid State Ionics* **9/10,** 153 (1983).
5. R. KANNO, Y. TAKEDA, K. TAKADA, AND O. YAMAMOTO, *J. Electrochem. Soc.* **131,** 469 (1984).

6. C. J. J. van Loon and J. de Jong, *Acta Crystallogr. Sect. B* **31,** 2549 (1975).
7. L. Hanebali, T. Machej, C. Cros, and P. Hagenmuller, *Mater. Res. Bull.* **16,** 887 (1981).
8. L. Latie, G. Villeneuve, C. Cros, and P. Hagenmuller, *Phys. Status Solidi, B* **128,** 475 (1985).
9. H-J. von Seifert, *Z. Anorg. Allg. Chem.* **307,** 137 (1961).
10. R. Kanno, Y. Takeda, A. Takahashi, O. Yamamoto, R. Suyama, and S. Kume, *J. Solid State Chem.* **71,** 196 (1987).
11. F. Izumi, *J. Miner. Soc. Japan* **17,** 37 (1985). [in Japanese]
12. G. Villeneuve, L. Latie, C. Cros, and P. Hagenmuller, *Mater. Res. Bull.* **19,** 1515 (1984).
13. C. J. J. van Loon and D. J. Ijdo, *Acta Crystallogr. B* **31,** 770 (1975).
14. A. B. Lidiard, *in* "Encyclopedia of Physics" (W. Jost, Ed.), Vol. 10, pp. 246–349. Springer, Berlin (1956).
15. N. Bonanos and E. Lilley, *Solid State Ionics* **1,** 223 (1980).
16. L. Hanebali, These de Doctorat d'Etat, Univ. Bordeaux I (1983).
17. R. Kanno, Y. Takeda, O. Yamamoto, C. Cros, W. Gang, and P. Hagenmuller, *Solid State Ionics* **20,** 99 (1986).